HTML ABSTRACT + LINKS

Role of step edges in oxygen vacancy transport into $SrTiO_3$(001)

X. D. Zhu[a)]
Department of Physics, University of California at Davis, Davis, California 95616

Y. Y. Fei, H. B. Lu, and G. Z. Yang
Beijing National Laboratory for Condensed Matter Physics, Institute of Physics, Chinese Academy of Sciences, Box 603, Beijing 100080, China

(Received 4 May 2005; accepted 13 June 2005; published online 25 July 2005)

Using a combination of oblique-incidence optical reflectivity difference and *specular* reflection high energy electron diffraction techniques, we studied vacuum annealing of pulsed-laser deposited Nb-doped $SrTiO_3$ monolayers on $SrTiO_3$(100) near 730 °C. In *oxygen-free* ambient, the as-grown monolayers are oxygen deficient. The excess oxygen vacancies in the monolayers are reduced by vacancy diffusion into the bulk. We found that the reduction rate is characterized by an activation energy $E=1.0$ eV. More interestingly, the pre-exponential factor decreases significantly as the annealing time interval increases between two successive monolayer depositions. We propose that the *indiffusion* of excess surface oxygen vacancies takes place at step edges, and the Oswald ripening governs the density of the latter during vacuum annealing. © *2005 American Institute of Physics*. [DOI: 10.1063/1.2005398]

Heterostructures of perovskite oxides have emerged as promising materials for material research and device applications. The structure compatibility has enabled successful fabrication of epitaxial heterostructures of these oxides. Since perovskite oxides take on a wide range of properties (e.g., insulators, superconductors, ferromagnets, ferroelectrics, optically nonlinear crystals), integration and interplay of these properties through properly grown heterostructures promise exciting materials and new device application. As demonstrated by Hwang *et al.* and others, heterostructures of perovskite oxides with high degree of crystallinity and interfaces as sharp as one molecular layer can be fabricated with pulsed laser deposition (PLD) and reactive molecular beam epitaxy.[1–3] In addition to crystallinity, properties of oxide films are subject to oxygen content.[4–6] Films grown under pulsed-laser-deposition conditions are typically oxygen deficient, even when the deposition is carried out in oxygen ambient. Excess oxygen vacancies in as-grown oxide films are usually removed by post-growth annealing in oxygen-rich ambient.[7–9] Understanding the mechanisms and kinetic details of oxidation reactions is essential for preparation stoichiometry oxide films.

In oxygen-free ambient, driven by chemical potential disparity, excessive oxygen vacancies in as-grown oxide films diffuse into the bulk so that the films still become oxidized even at typical growth temperatures.[10] Though the indiffusion of excess surface oxygen vacancies can take place on terraces or preferentially at chemically active sites such as step edges, our investigation shows that the latter is the case. In this letter we report the findings of such an investigation.

The experiment was carried out in a pulsed laser deposition chamber with a base pressure of 1×10^{-5} Pa (7.5×10^{-8} Torr). The chamber is equipped with a standard reflection high-energy electron diffraction (RHEED) apparatus and an oblique-incidence optical reflectance difference measurement system.[10] The $SrTiO_3$(001) substrate of $10\times5\times0.5$ mm^3 is attached to a stainless heater block. The substrate temperature is monitored with an optical pyrometer. A sintered ceramics of stoichiometric Nb:$SrTiO_3$ (10 mol %) is used as the target. A 308-nm XeCl excimer laser at a repetition rate of 2 Hz is used for ablation. We deposit one monolayer of Nb:$SrTiO_3$ at a time in oxygen-free ambient using 38 laser pulses. At the completion of one monolayer, we interrupt the deposition and continue to monitor the properties of the as-deposited monolayer. In particular, we examine how the reduction rate of excess oxygen vacancies varies with temperature and the annealing time interval between two successive monolayer depositions by monitoring the oblique-incidence optical reflectivity difference (OI-RD) from the growth surface.[7,8,10,11]

The experimental setup and procedures have been described previously. Briefly let r_{p0} and r_{s0} be the respective reflectivity from the bare substrate for *p*- and *s*-polarized light at the wavelength of a He–Ne probe laser $\lambda=632.8$ nm. Let r_p and r_s be the respective reflectivity during and after the deposition. Fractional changes in reflectivity are defined as $\Delta_p\equiv(r_p-r_{p0})/r_{p0}$ and $\Delta_s\equiv(r_s-r_{s0})/r_{s0}$. We measure the difference defined as $\Delta_p-\Delta_s$. Let $\varepsilon_d=\varepsilon_d'+i\varepsilon_d''$ be the optical dielectric constant of a Nb:$SrTiO_3$ monolayer. The measurable $\mathrm{Re}\{\Delta_p-\Delta_s\}$ is proportional to ε_d''.[8] For an as-deposited Nb:$SrTiO_3$ monolayer, ε_d'' comes from (1) an intrinsic absorption of a stoichiometric Nb:$SrTiO_3$, and (2) an extra absorption associated with the oxygen vacancies in the monolayer.[12,13] By monitoring $\mathrm{Re}\{\Delta_p-\Delta_s\}$, we follow the buildup and removal of excess oxygen vacancies.[8,10]

At substrate temperatures above 630 °C, even in an oxygen-free ambient, the specular RHEED intensity recovers to the predeposition level essentially right after a monolayer-equivalent of Nb:$SrTiO_3$ is deposited.[10] This shows that the deposited layer is recrystallized and "smooth" over the coherent length of the RHEED system. However the post-growth monolayer contains excess oxygen vacancies as revealed in the optical reflectivity difference signal. In Fig. 1, we display the measured $\mathrm{Re}\{\Delta_p-\Delta_s\}$ during and after the deposition at 730 °C and under a base pressure of 1×10^{-5} Pa. The three curves correspond to different time in-

a)Electronic mail: xdzhu@physics.ucdavis.edu

 © 2005 American Institute of Physics
Downloaded 12 Nov 2005 to 159.226.36.218. Redistribution subject to AIP license or copyright, see http://apl.aip.org/apl/copyright.jsp

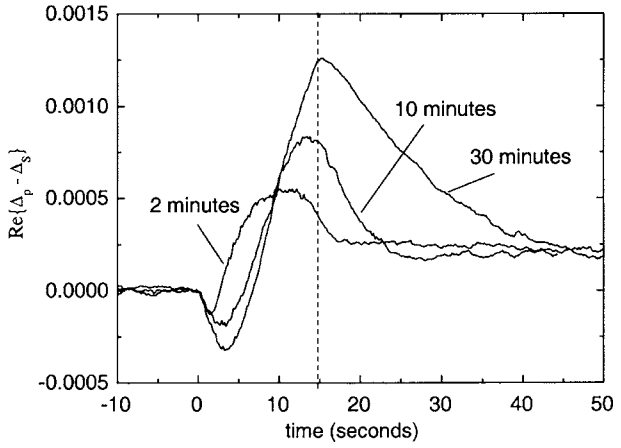

FIG. 1. Optical reflectivity difference $\mathrm{Re}\{\Delta_p - \Delta_s\}$ during and after an interrupted deposition of one $Nb:SrTiO_3$ monolayer on $SrTiO_3(001)$ in oxygen-free ambient at temperature of 730 °C. The time interval between two successive interrupted depositions varies from 2 to 30 min. The dotted line marks the completion of the deposition of one monolayer.

tervals between two successive monolayer depositions. At each time interval, $\mathrm{Re}\{\Delta_p - \Delta_s\}$ becomes reproducible (as displayed in Fig. 1) after a few successive depositions that are separated by the same time interval. $\mathrm{Re}\{\Delta_p - \Delta_s\}$ measures the optical absorption of the monolayer. The initial rise in absorption decreases during the thermal annealing and levels off to a value corresponding to that of a stoichiometric $Nb:SrTiO_3$ monolayer.[10] The extra absorption before leveling off comes from excess oxygen vacancies in the $Nb:SrTiO_3$ monolayer. Figure 1 shows that the excess oxygen vacancies are removed from the surface by vacancy diffusion into the bulk.

For annealing time intervals of 5 and 10 min, we further measured the recovery rates for $\mathrm{Re}\{\Delta_p - \Delta_s\}$ from 630 to 760 °C. By fitting the signal recovery to $\exp[-\alpha(T)t]$, we extracted the rate constant $\alpha(T)$. In Fig. 2, we display the Arrhenius plots of $\alpha(T)$. For both annealing time intervals, $\alpha(T)$ is a good Arrhenius function, $\alpha_0 \exp(-E/k_B T)$. The activation energies E are ~1.0 eV in both cases. The preexponential factor α_0 is 1.1×10^4 s^{-1} for 5-min time interval and 4.7×10^3 s^{-1} for 10-min time interval. Good Arrhenius behaviors and nearly identical activation energies indicate that the oxygen vacancy reduction is most likely rate limited by a single thermally activated process. More interestingly and as already illustrated in Fig. 1, the preexponential factor depends on the annealing time. *The longer two successive monolayer depositions are separated, the smaller the preexponential factor is*. This peculiar dependence on annealing time interval rules out transport of excess oxygen vacancies directly from flat terraces into the bulk. This is because that according to the specular RHEED, the growth surface is more or less smooth right after the deposition and therefore the coverage of flat terraces does not change significantly with the length of the annealing time interval. We note though that the step density continues to change due to Oswald ripening.

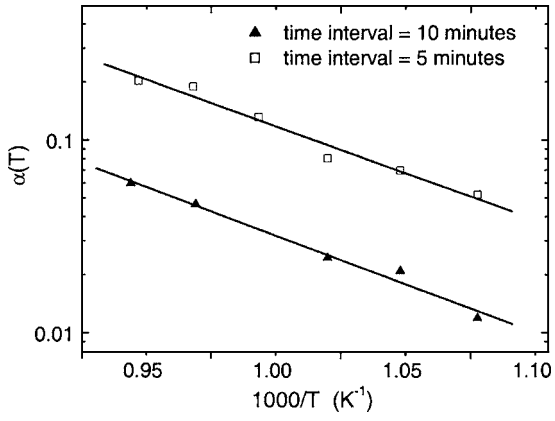

FIG. 2. Arrhenius plots of the optical signal recovery rates $\alpha(T)$ with annealing time interval set to 5 and 10 min. Solid lines are fit to $\alpha_0 \exp(-E/k_B T)$.

We now explore the mechanism that is responsible for the dependence of the excess oxygen vacancy reduction on thermal annealing time. In a study of pulsed laser deposition of $SrTiO_3$ on $SrTiO_3(100)$ using surface x-ray diffraction (SXRD), Eres and co-workers reported that the off-specular intensity goes through a momentary change after each ablation pulse. It dips sharply right after the pulse and subsequently tends to recover to an equilibrium level before the next ablation pulse. The initial dip is more pronounced and takes longer to recover when the coverage of the deposit θ is close to zero (in the beginning) or close to a full monolayer (near the end of a monolayer deposition). The change was attributed to out-of-registry surface reconstructions induced by surface oxygen vacancies.[14] The recovery from such a change is then expected to follow the density of excess surface oxygen vacancies.[15] From our present study, it should in turn depend on the surface morphology through the coverage. In the study of Eres *et al.*, the growth of $SrTiO_3$ proceeds in a nearly perfect layer-by-layer mode such that the density of step edge atoms θ_s varies with the deposit coverage θ as $(1-\theta)\sqrt{-\mathrm{Ln}(1-\theta)}$.[16] The recovery of their off-specular SXRD qualitatively follows this trend.[15]

We propose that transport of excess surface oxygen vacancies into a bulk $SrTiO_3$ crystal takes place at or near step edges; either the surface diffusion towards step edges or the indiffusion at step edges determines the reduction rate of the oxygen vacancies. This mechanism operates independently from the oxidation reaction with ambient oxygen (through a precursor-state as reported by Zhu *et al.* and Tanaka *et al.*[8]). It explains why the preexponential factor in the excess oxygen vacancy reduction rate depends on the annealing time. As we show below, the steady-state density of step edge atoms is governed by the balance between the post-growth Oswald ripening and the accumulation of small-radius islands during each monolayer deposition, and thus decreases with increasing annealing time interval. It also qualitatively explains the off-specular surface x-ray diffraction intensity recovery as reported by Eres *et al.*

Even in a layer-by-layer growth, a post-growth surface contains a distribution of two-dimensional (2D) islands (or clusters) and shallow three-dimensional (3D) islands. It usually takes the growth surface a long time (compared to the time needed for depositing a monolayer) to become flat with terraces determined only by the miscut angle.[17,18] Driven by the Gibbs–Thompson effect, small islands decompose while large islands grow through Oswald ripening so that the mean radius $r(t)$ of the island distribution increases with time as $r(t) \sim (1 + t/\tau_c)^{1/3}$.[19] τ_c is a decreasing function of temperature. If Oswald ripening is governed by surface diffusion of unit cells, $\tau_c \sim \exp(E_{\mathrm{diff}}/k_B T)$ with E_{diff} being the energy barrier for unit cell diffusion on terraces. On average one ex-

Downloaded 12 Nov 2005 to 159.226.36.218. Redistribution subject to AIP license or copyright, see http://apl.aip.org/apl/copyright.jsp

pects the density of step edge atoms to be approximately $\theta_s \sim 1/r(t) \sim (1+t/\tau_c)^{-1/3}$. Starting from a smooth substrate surface, the deposition of one monolayer-equivalent $Nb:SrTiO_3$ increases the density of small-radius islands slightly. If the time interval τ between two successive monolayer depositions is long so that Oswald ripening is completed, the density of step edge atoms will remain small. If the time interval τ is insufficient, the islands with small radii will accumulate. The accumulation stops when Oswald ripening, whose rate increases with the density of small-radius islands, balances the net accumulation from one monolayer deposition. We then have a steady-state density of islands with a mean radius r_τ, and the density of step edge atoms is given by $\theta_s \sim 1/r_\tau$. The shorter the annealing time interval is, the smaller r_τ and the larger the density of step edge atoms $\theta_s \sim 1/r_\tau$. When the indiffusion of oxygen vacancies takes place at step edges, we expect the reduction rate to decrease when the annealing time interval is lengthened. This is what we observed.

It is well known that the bulk diffusion rate for oxygen vacancies in an unannealed $SrTiO_3$ crystal is higher than in an annealed $SrTiO_3$ crystal.[20,21] This was attributed to the dislocation-assisted diffusion of oxygen vacancies in the unannealed crystal. Our indirect observation of step edges serving to facilitate indiffusion for excess oxygen vacancies is a surface manifestation of defect-assisted oxygen vacancy transport. Step edges as sources as well as sinks for material transport in and out of a bulk crystal have also been observed indirectly on NiAl(110) by McCarty and co-workers[22] and on Co/Cu(100) by Schmid and co-workers.[23]

In conclusion, we find that step edges act as pathways for excess oxygen vacancies in $Nb:SrTiO_3$ monolayers to diffuse into the bulk of the substrate during vacuum annealing. Depending upon whether surface diffusion to or indiffusion at the step edges dominates, the reduction rate of excess oxygen vacancies is expected to vary quadratically or linearly with the density of step edge atoms, θ_s.

The authors acknowledge the support for this work by the Chinese Natural Science Foundation. X.D.Z. also acknowledges support in part by the donor of Petroleum Research Fund, administered by American Chemical Society.

[1] A. Ohtomo, D. A. Muller, J. L. Grazul, and H. W. Hwang, Nature (London) **419**, 378 (2002).
[2] D. G. Schlom, J. H. Haeni, C. D. Theis, W. Tian, X. Q. Pan, G. W. Brown, and M. E. Hawley, Mater. Res. Soc. Symp. Proc. **219**, 105 (2000).
[3] Y. Guozhen, L. Huibin, W. Hui-Sheng, C. D.-Fu, Y. H.-Qing, W. H. Z. Yueliang, and C. Zheng-H., Chin. Phys. Lett. **14**, 478 (1997).
[4] H. L. Ju, J. Gopalakrishnan, J. L. Peng, Q. Li, G. C. Xiong, T. Venkatesan, and R. L. Greene, Phys. Rev. B **51**, 6143 (1995).
[5] J. P. Sydow, R. A. Ruhrman, and B. H. Moeckly, Appl. Phys. Lett. **72**, 3512 (1998).
[6] R. Waser and D. M. Smyth, in *Ferroelectric Thin Films: Synthesis and Basic Properties*, edited by C. P. de Araujo, J. F. Scott, and G. W. Taylor (Gordon and Breach, Amsterdam, 1996), p. 47.
[7] X. D. Zhu, W. Si, X. X. Xi, Q. Li, Q. D. Jiang, and M. G. Medici, Appl. Phys. Lett. **74**, 3540 (1999).
[8] X. D. Zhu, W. Si, X. X. Xi, and Q. D. Jiang, Appl. Phys. Lett. **78**, 460 (2001); H. Tanaka, T. Matsumoto, T. Kawai, and S. Kawai, Surf. Sci. **318**, 29 (1994).
[9] W. S. Epling, C. H. F. Peden, M. A. Henderson, and U. Diebold, Surf. Sci. **412–413**, 333 (1998).
[10] F. Chen, T. Zhao, Y. Y. Fei, H. B. Lu, Z. H. Chen, G. Z. Yang, and X. D. Zhu, Appl. Phys. Lett. **80**, 2889 (2002).
[11] X. D. Zhu, H. B. Lu, G. Z. Yang, Z. Y. Li, B. Y. Gu, and D. Z. Zhang, Phys. Rev. B **57**, 2514 (1998).
[12] T. Higuchi, T. Tsukamoto, K. Kobayashi, Y. Ishiwata, M. Fujisawa, T. Yokoya, S. Yamaguchi, and S. Shin, Phys. Rev. B **61**, 12860 (2000).
[13] A. Hirata, A. Ando, K. Saiki, and A. Koma, Surf. Sci. **310**, 89 (1994).
[14] J. Zegenhagen, T. Haage, and Q. D. Jiang, Appl. Phys. A **67**, 711 (1998).
[15] G. Eres, J. Z. Tischler, M. Yoon, B. C. Larson, C. M. Rouleau, D. H. Lowndes, and P. Zschack, Appl. Phys. Lett. **80**, 3379 (2002).
[16] S. Stoyanov and M. Michailov, Surf. Sci. **202**, 109 (1988).
[17] J. A. Stroscio, D. T. Pierce, and R. A. Dragoset, Phys. Rev. Lett. **70**, 3615 (1993); J. A. Stroscio and D. T. Pierce, J. Vac. Sci. Technol. B **12**, 1783 (1994).
[18] M. C. Bartelt and J. W. Evans, Phys. Rev. Lett. **75**, 4250 (1995).
[19] M. Zinke-Allmang, L. C. Feldman, and M. H. Grabow, Surf. Sci. Rep. **16**, 377 (1992).
[20] A. E. Paladino, J. Am. Ceram. Soc. **48**, 476 (1965); A. E. Paladino, L. G. Rubin, and J. S. Waugh, J. Phys. Chem. Solids **26**, 391 (1965).
[21] S. Zafer, R. E. Jones, B. Jiang, B. White, P. Chu, D. Taylor, and S. Gillespie, Appl. Phys. Lett. **73**, 175 (1998).
[22] K. F. McCarty, J. A. Nobel, and N. C. Bartelt, Nature (London) **412**, 622 (2001).
[23] A. K. Schmid, D. Atlan, H. Itoh, B. Heinrich, T. Ichinokawa, and J. Kirschner, Phys. Rev. B **48**, 2855 (1993).

Downloaded 12 Nov 2005 to 159.226.36.218. Redistribution subject to AIP license or copyright, see http://apl.aip.org/apl/copyright.jsp